Enhanced antitumor activity of P450 prodrug-based gene therapy using the low K_m cyclophosphamide 4-hydroxylase P450 2B11

Youssef Jounaidi, Chong-Sheng Chen, Gareth J. Veal, and David J. Waxman

Division of Cell and Molecular Biology, Department of Biology, Boston University, Boston, Massachusetts

Abstract

Gene therapy using the prodrug-activating enzyme P450 2B6 has shown substantial promise in preclinical and initial clinical studies with the P450 prodrugs cyclophosphamide and ifosfamide. We sought to optimize this therapy using the canine P450 enzyme 2B11, which activates cyclophosphamide and ifosfamide with K_m of 80 to 160 μmol/L, ~10- to 20-fold lower than the K_m of P450 2B6. Retrovirus encoding a P450 2B11-internal ribosome entry signal-P450 reductase expression cassette induced marked cyclophosphamide and ifosfamide cytotoxicity toward 9L gliosarcoma cells and exhibited an impressive bystander killing effect at micromolar prodrug concentrations, where P450 2B6 displayed low activity. Adeno-2B11, a replication-defective, E1/E3 region-deleted adenovirus engineered to coexpress P450 2B11 and P450 reductase, dramatically increased tumor cell-catalyzed cyclophosphamide 4-hydroxylation and cytotoxicity compared with Adeno-2B6 and effected strong bystander killing at low (20 μmol/L) cyclophosphamide concentrations. Further increases in cyclophosphamide cytotoxicity were obtained in several human cancer cell lines, including a 4-hydroperoxycyclophosphamide-resistant MCF-7 breast cancer cell line, when Adeno-2B11 was combined with Onyx-017, an E1b-55-kDa gene-deleted, tumor cell-replicating adenovirus that coamplifies and facilitates tumor cell spread of Adeno-2B11. To evaluate the therapeutic effect of P450 2B11 expression *in vivo*, 9L gliosarcoma cells transduced with P450-expressing retrovirus were grown as solid s.c. tumors in immunodeficient mice. Cyclophosphamide treatment on a metronomic, 6-day repeating schedule led to full regression of 9L/2B11 tumors but not P450-deficient control tumors, resulting in a tumor-free period lasting up to ~100 days. 9L/2B6 tumors regressed more slowly and exhibited a tumor-free period of only 21 to 39 days. Thus, P450 gene-directed enzyme prodrug therapy can be greatly improved by using the low K_m P450 enzyme 2B11, which catalyzes intratumoral activation of cyclophosphamide and ifosfamide at pharmacologically relevant drug concentrations. [Mol Cancer Ther 2006;5(3):541–55]

Introduction

Gene-directed strategies that increase the chemosensitivity of tumor cells by stimulating tumor cell-catalyzed activation of anticancer prodrugs offer a unique opportunity to improve the efficacy of cancer chemotherapeutic agents (1–3). These gene-directed enzyme prodrug therapies (GDEPT) use a variety of anticancer prodrugs, including agents activated by bacterial, viral, and mammalian enzymes. Tumor-selective delivery of a prodrug activation gene can be achieved in a variety of ways, including the use of viral vectors that incorporate tumor-specific promoters (4) or selectively replicate in tumor cells that present specific genetic defects, such as p53 deficiency (5), or are characterized by pathophysiologic conditions, such as hypoxia (6). One GDEPT strategy uses genes that encode mammalian cytochrome P450 enzymes (7, 8), which metabolize anticancer prodrugs, including the oxazaphosphorines cyclophosphamide and ifosfamide, to active, cytotoxic metabolites (9, 10). Prodrug-activating P450 enzymes are expressed at high levels in liver but are generally deficient or present at very low levels in human tumors (11–14). Consequently, substantial increases in intratumoral production of active drug metabolites and enhanced anticancer activity may be realized by delivery of prodrug activation P450 genes to tumor cells (9, 15, 16).

Cyclophosphamide is commonly given in combination with other chemotherapeutic drugs in both adjuvant and high-dose chemotherapy settings and shows considerable clinical activity against a broad range of tumors, including breast cancer, endometrial cancer, and various leukemias and lymphomas (17). Preclinical P450 GDEPT studies using cyclophosphamide have shown a substantial improvement in antitumor activity associated with a decrease in systemic toxicity compared with conventional chemotherapy. An important feature of this P450-based gene therapy is its use of established, clinically effective anticancer prodrugs, such as cyclophosphamide, whose active 4-hydroxy-metabolite exerts bystander cytotoxicity that is not limited to immediately adjacent tumor cells (8, 18). Further enhancement of P450 GDEPT can be obtained by coexpression of P450 with the flavoenzyme NADPH P450 reductase (P450R; refs.

Received 8/12/05; revised 12/5/05; accepted 1/11/06.

Grant support: NIH grant CA49248 (D.J. Waxman).

The costs of publication of this article were defrayed in part by the payment of page charges. This article must therefore be hereby marked advertisement in accordance with 18 U.S.C. Section 1734 solely to indicate this fact.

Author Correspondence: Youssef Jounaidi or David J, Waxman, Division of Cell and Molecular Biology, Department of Biology, Boston University, 5 Cummington Street, Boston, MA 02215. Fax: 617-353-7404. E-mail: jounaidi@bu.edu or djw@bu.edu

doi:10.1158/1535-7163.MCT-05-0321

18, 19), by combination of cyclophosphamide with other prodrugs, including P450/P450R-activated bioreductive drugs (20, 21), and by administration of cyclophosphamide using a metronomic schedule (22), which is associated with antiangiogenic activity (23). P450 gene transfer can be achieved both in cell culture and in human xenograft models by using tumor cell replication-conditional herpesvirus (24, 25) or adenovirus vectors (26) to effect efficient, tumor-selective P450 gene delivery. Recent phase I/II clinical trials support the clinical development of P450 GDEPT based on studies using cellular vectors to deliver P450 2B1 to advanced pancreatic cancer patients treated with ifosfamide (27, 28) and retroviral vectors to deliver P450 2B6 to advanced breast cancer and melanoma patients given oral cyclophosphamide (29).

P450 enzymes, such as P450 2B1 and P450 2B6, metabolize many drug substrates, including cyclophosphamide and ifosfamide, with a high K_m, in the millimolar range (30, 31). High drug concentrations are therefore required for efficient prodrug activation and bystander tumor cell killing, limiting the utility of P450 GDEPT. Enhanced enzyme activity may potentially be achieved by using a low K_m P450 enzyme, which could lead to increased activity at the sub-K_m plasma levels of cyclophosphamide and ifosfamide typically seen in cancer patients (32, 33). We have recently identified a canine enzyme, P450 2B11, as a low K_m catalyst of cyclophosphamide and ifosfamide activation whose kinetic properties in an *in vitro* reconstituted enzyme system (K_m, 80–160 μmol/L; ref. 34) are far superior to those of P450 2B6 (K_m, ~1,900 μmol/L; ref. 31). It is not clear, however, whether the low K_m of P450 2B11 will be manifest in the environment of an intact cell or whether a low K_m will translate into improved GDEPT activity in an animal tumor model *in vivo*.

Presently, we investigate whether efficient activation of cyclophosphamide and ifosfamide and effective tumor cell killing can be achieved at micromolar prodrug concentrations by introduction of P450 2B11 in combination with P450R and whether further increases in antitumor activity can be obtained by combining a replication-defective adenoviral vector encoding P450 2B11 and P450R with Onyx-017 (26), a replication-conditional oncolytic adenovirus. We also evaluate the effect of retroviral expression of P450 2B11 in a *scid* mouse tumor xenograft model and, in the context of an intact liver, on the therapeutic responses to cyclophosphamide compared with those seen with P450 2B6. Our findings establish that P450 2B11, with its low K_m and high catalytic efficiency, has the potential to substantially improve the utility of P450 GDEPT applications for cancer treatment.

Materials and Methods

Materials

Cyclophosphamide, chloroquine, and puromycin were purchased from Sigma Chemical Co. (St. Louis, MO). 4-OH-cyclophosphamide and 4-OH-ifosfamide, chemically activated derivatives of cyclophosphamide and ifosfamide, respectively, were obtained from Dr. Ulf Niemeyer (Baxter Oncology GmbH, Frankfurt, Germany). Fetal bovine serum (FBS) and DMEM were purchased from Life Technologies (Grand Island, NY). The conditional-replicating adenovirus Onyx-017 (26) was obtained from Onyx Pharmaceuticals, Inc. (Richmond, CA). Human tumor cell lines U251 (brain), PC-3 (prostate), and MCF-7 (breast) were obtained from Dr. Dominic Scudiero (National Cancer Institute, Bethesda, MD; ref. 35). MCF-7/4HC cells, which display ~6-fold resistance to activated cyclophosphamide (4-OH-cyclophosphamide), are described elsewhere (36). Human tumor cells were grown at 37°C in a humidified, 5% CO_2 atmosphere in RPMI 1640 containing 5% FBS, 100 units/mL penicillin, and 100 μg/mL streptomycin. Rat 9L gliosarcoma cells were grown in DMEM containing 10% FBS and antibiotics.

Retroviral Plasmid Construction

The retroviral plasmids pBabe-2B6-P450R-puro (26), pBabe-2B1-P450R-puro, and pBabe-2B11-P450R-puro are based on the pBabe series (37), which contains a puromycin resistance gene transcribed from an internal SV40 promoter. These retroviruses generate a bicistronic mRNA transcribed from the 3′-long terminal repeat of the viral vector, which encodes the indicated P450 2B cDNA linked to human P450R cDNA by an internal ribosome entry signal (IRES). pBabe-2B1-P450R-puro was constructed by excising the rat P450 2B1 coding sequence from pBabe-2B1-puro (38) using *Eco*RI and *Apo*I followed by ligation of the fragment to the *Eco*RI site of pBabe-IRES-P450R-puro (26). pBabe-2B11-P450R-puro was constructed by excising the P450 2B11 coding sequence, including 147 bp of 3′-untranslated region sequence, from plasmid pCD39 (Dr. James R. Halpert, University of Texas Medical Branch, Galveston, TX; ref. 39) using *Eco*RI and *Apo*I followed by subcloning into the *Eco*RI site of pBabe-IRES-P450R-puro.

9L Cell Lines Coexpressing P450 and P450R cDNAs (9L/P450 Cells)

Transfection of the ecotropic packaging cell line Bosc 23 (40) with the above-described pBabe-2B-P450R-puro plasmids, harvesting of retroviral supernatants, and infection of rat 9L gliosarcoma cells were carried out as detailed elsewhere (18, 41), with the following modifications. Bosc 23 cells were plated at 2.5×10^6 in a 60-mm dish. Fresh medium (4 mL) containing chloroquine (25 μmol/L) was added to the cells 16 hours later. The cells were cotransfected 1 hour later with 40 μg pBabe-derived plasmid DNA and 7.5 μg pKat (42) using a calcium phosphate precipitation method. Pools of cells resistant to puromycin (2.5 μg/mL) were selected beginning 48 hours later over a 2- to 3-day period (18) with an overall survival rate of >80%. The resultant drug-resistant pools of 9L/P450 cells were propagated, lysed by sonication, and then assayed for P450R-catalyzed, NADPH-dependent cytochrome *c* reduction (ΔA_{550}) at 30°C in 0.3 mol/L potassium phosphate buffer (pH 7.7) containing 0.525 mg/mL cytochrome *c*. 9L cells infected with empty pBabe retrovirus (9L/pBabe cells, also called 9L control cells) served as P450-deficient controls. P450 protein expression was

verified in each 9L/P450 cell pool by Western blot analysis of 50 μg sonicated cell lysate protein using rabbit anti-P450 2B1 polyclonal antibody. Lymphoblast-expressed P450 2B1 and P450 2B6 (BD-Gentest, Inc., Woburn, MA) and bacterial-expressed P450 2B11 (34) were used as standards.

9L/P450 Cell Growth Inhibition Assay

The chemosensitivity of 9L/P450 cells was determined using a 4-day growth inhibition assay. Cells were plated overnight in triplicate at 4,000 per well of a 48-well plate. The cells were then treated for 4 days with cyclophosphamide at concentrations specified in each experiment. Cells remaining at the end of day 4 were stained and quantified using a crystal violet/alcohol extraction assay (18). Data are expressed as cell number (A_{595}) relative to drug-free controls, mean ± SD for triplicate samples, unless indicated otherwise. Effective drug concentrations for 50% response (EC_{50}) were determined based on incubations with cyclophosphamide or ifosfamide (0–120 μmol/L for 9L/2B11 cells and 0–1,000 μmol/L for 9L/2B1 and 9L/2B6 cells). Sigmoidal dose-response analysis using a variable slope was done using the nonlinear regression curve fit program of GraphPad Prism (GraphPad Software, San Diego, CA). Data were plotted as percentage of cells killed versus $\log_{10}$ of the molar concentration of cyclophosphamide and ifosfamide.

Assay for 4-OH-Cyclophosphamide Formation by 9L/P450 Cells

Apparent K_m and V_{max} values for 9L/P450 cell-catalyzed cyclophosphamide and ifosfamide 4-hydroxylation were determined as follows. Cells (1×10^5) were seeded in 12-well plates and grown for 48 hours. Cells were treated for 4 hours with 0 to 6 mmol/L cyclophosphamide or ifosfamide in 2 mL culture medium containing 5 mmol/L semicarbazide to trap the 4-hydroxy-metabolite.

Aliquots of medium (500 μL) were removed and treated with $ZnSO_4$ and $Ba(OH)_2$ to precipitate protein and then derivatized to 7-hydroxyquinoline by treatment for 25 minutes at 90°C with 100 μL freshly prepared fluorescent reagent (60 mg 3-aminophenol and 60 mg hydroxylamine-HCl in 10 mL of 1 N HCl). Samples were analyzed by high-performance liquid chromatography (HPLC) and quantified by comparison with standard curves of metabolite prepared using 4-OOH-cyclophosphamide dissolved in culture medium (43, 44). In some cases, the derivatized samples were stored at −20°C in the dark before HPLC analysis.

Evaluation of Bystander Activity

Mixtures of wild-type 9L cells and 9L/P450 cells containing increasing percentages of 9L/2B6, 9L/2B1, or 9L/2B11 cells (0%, 5%, 10%, 20%, and 100% of total cells) were plated overnight in 1 mL culture medium to give a total of 10^5 cells per well of a 12-well plate. The cells were then treated with cyclophosphamide for a total of 96 hours, with the cyclophosphamide-containing culture medium changed after the first 48 hours. Cells were then stained and quantified using the crystal violet assay described above.

Construction and Purification of Recombinant Adenoviruses

Adeno-2B6, a replication-defective, E1/E3 region-deleted adenovirus encoding P450 2B6 linked to P450R via an IRES sequence, was described previously (26). A corresponding adenovirus expressing P450 2B11 and P450R (Adeno-2B11) was constructed using the Adeno-X expression system (Clontech Labs, Inc., Palo Alto, CA). Retroviral plasmid pBabe-2B11-P450R-puro was linearized using *Eco*RI, blunt ended, and the P450 2B11-IRES-P450R expression cassette was then excised with *Dra*I and ligated into the *Dra*I site of pShuttle (Clontech Labs). The resulting plasmid, pShuttle-2B11-P450R, was used to construct the recombinant adenovirus, Adeno-2B11, as described by the manufacturer. The cytomegalovirus immediate-early promoter of pShuttle drives Adeno-2B11-directed expression of P450 2B11 and P450R and ensures robust expression in a wide range of cell lines and tissues. The functionality of Adeno-2B11 was initially determined by assaying P450R activity (cytochrome *c* reduction) in cell lysate prepared from Adeno-2B11-infected human kidney HEK 293 cells. Typically, a 4-fold increase in P450R activity was observed 48 hours postinfection when compared with cells infected with a control replication-defective adenovirus, adeno-*Pme*I (constructed with the empty pShuttle vector of Adeno-X system).

Adenoviral stocks were propagated in HEK 293 cells grown in 100-mm dishes at 37°C in a humidified 5% CO_2 incubator in DMEM containing 25 mmol/L glucose, 100 units/mL penicillin, 100 μg/mL streptomycin, and 10% heat-inactivated FBS (26). The purified virus was desalted by dialysis at 4°C against 10 mmol/L Tris (pH 8.0), 1 mmol/L $MgCl_2$, and 10% glycerol. The effectiveness of desalting was verified by conductivity measurements. Viral titers were determined as described in the Adeno-X Rapid Titer kit manual (Clontech Labs) and typically ranged from 10^{10} to 10^{11} plaque-forming units/mL for both adeno-P450 viruses. Purified virus was stored in aliquots at −80°C.

P450R Activity, Cyclophosphamide 4-Hydroxylation, and Cytotoxicity in Adeno-P450-Infected Tumor Cells

U251 cells were seeded overnight in six-well plates at 10^5 per well and then infected for 3 to 4 hours with Adeno-2B6 or Adeno-2B11 in 1 mL RPMI 1640 containing 5% FBS at multiplicities of infection (MOI) of 25, 50, or 100 plaque-forming units/cell. Each adeno-P450 virus was used at MOI 12 in experiments involving coinfection with the tumor cell-replicating adenovirus Onyx-017 (26). Fresh culture medium (2 mL) was then added without changing the medium, and the incubation with virus was continued for ~20 hours. The cells were then changed to virus-free culture medium followed by an additional 24 hours incubation. The cells were then either (*a*) washed with PBS and lysed by sonication in 50 mmol/L potassium phosphate buffer (pH 7.4) containing 1 mmol/L EDTA and 20% glycerol and the lysates were assayed for P450R activity as described above for 9L cells or (*b*) the cells were treated for 4 hours with 100 or 250 μmol/L cyclophosphamide in 3 mL fresh RPMI 1640 containing 5% FBS and 5 mmol/L semicarbazide. Aliquots of culture medium (500 μL) were then removed and assayed for 4-OH-cyclophosphamide by HPLC as described above.

Cell lines used for cytotoxicity experiments (U251, PC-3, MCF-7, and MCF-7/4HC) were seeded in 24-well plates at

14,000 cells per well and allowed to establish growth overnight. The cells were then infected for 3 to 4 hours with Adeno-2B6 or Adeno-2B11 at MOI 0, 10, 25, or 50 in 0.2 mL RPMI 1640 containing 5% FBS. Fresh culture medium (0.8 mL) was then added followed by incubation with the virus for an additional 20 hours. The culture medium was then removed and the cells were treated with various concentrations of cyclophosphamide in 1 mL fresh RPMI 1640 containing 5% FBS. After 2 days of cyclophosphamide treatment, the medium was replaced with 1 mL fresh cyclophosphamide-containing culture medium for an additional 4 days. Cells remaining at the end of the 6-day cyclophosphamide treatment period were stained with crystal violet and quantified (A_{595}) as percent cell survival relative to drug-free controls. In experiments where the cells were infected by adeno-P450 in combination with Onyx-017, the levels of Adeno-2B6 and Adeno-2B11 were decreased to MOI 6 (for MCF-7 cells), MOI 8 (for U251 cells), or MOI 32 (for MCF-7/4HC and PC-3 cells).

The bystander activity of Adeno-2B11 was evaluated by infection of U251 cells, plated at 3×10^4 per well in 24-well plates 24 hours before infection with Adeno-2B11 (MOI 0 or 25) for a total of 20 to 24 hours as described above. Cells were then placed in fresh medium with or without 20 μmol/L cyclophosphamide for 2 days, at which time fresh medium ± cyclophosphamide was reapplied for an additional 5 days. Cells cultured for 2 days after removal of the adenovirus were fixed in 4% paraformaldehyde for 30 minutes and then washed twice for 5 minutes with PBS for immunostaining with anti-P450 2B11 antibody.

Samples were blocked with 3% FBS in PBS for 20 minutes. Anti-P450 2B11 antibody (kindly provided by Dr. James R. Halpert; 1:1,000 dilution in PBS containing 3% FBS) was applied to the cells for 1 hour at 37°C in a volume of 300 μL. The cells were then washed with PBS twice for 5 minutes. Secondary anti-rabbit antibody (1:500 dilution in PBS containing 3% FBS) was applied to the cells for 1 hour at 37°C. Cells were washed twice with PBS and P450 2B11-positive staining was visualized with the TMB substrate kit for peroxidase (Vector Laboratories, Burlingame, CA). P450 2B11-stained cells were then counted as a percentage of the overall U251 population. Cells were also stained with crystal violet to determine cell survival after 7 days of cyclophosphamide exposure.

Real-time PCR

Total RNA was isolated using TRIzol reagent according to the manufacturer's instructions for monolayer cells. Reverse transcription to yield cDNA was carried out using GeneAmp RNA core kit (Applied Biosystems, Foster City, CA) using 1 μg total RNA in a volume of 20 μL according to the manufacturer's instruction. cDNA (4 μL; 1:50 dilution) in a total volume of 16 μL SYBR Green and PCR primers mixture was used for quantitative real-time PCR with the following primers: 5′-AAATCCTTCCTCAGGCTCCAA-3′ (P450 2B11 sense primer), 5′-GCCTCCCGTATGGCGTC-TAT-3′ (P450 2B11 antisense primer), 5′-TTACAGTGCT-CGCTTTGGTCTGT-3′ (adenovirus E3 sense primer), and 5′-TAAAGCTGCGTCTGCTTTTGTATTT-3′ (adenovirus E3 antisense primer). Samples were incubated at 95°C for 10 minutes followed by 40 cycles of 95°C for 15 seconds and 60°C for 1 minutes in an ABI PRISM 7900HT Sequence Detection System (Applied Biosystems). Results were analyzed using the comparative C_T ($\Delta\Delta C_T$) method as described by the manufacturer. Data are presented as fold increase of each RNA compared with uninfected cell controls after normalization for the 18S RNA content of each sample.

Evaluation of Antitumor Activity in Tumor Xenografts Grown in *scid* Mice

Seven-week-old (25 to 29 g) male ICR/Fox Chase *scid* mice (Taconic Farms, Germantown, NY) were injected s.c. at each posterior flank with 4×10^6 9L/pBabe cells (control), 9L/2B6 cells, or 9L/2B11 cells in 0.5 mL serum-free DMEM using a 0.5-inch 29-gauge needle and a 1 mL insulin syringe. Tumor areas (length × width) were measured twice weekly using Vernier calipers (Manostat Corp., Herisau, Switzerland) and tumor volumes were calculated based on the following formula: volume = π / 6 (length × width)$^{3/2}$. When the tumors reached ~1,000 to 1,200 mm^3 in volume (23 days after tumor implantation), the mice were treated with cyclophosphamide using a metronomic schedule, 140 mg cyclophosphamide/kg body weight repeated every 6 days (22). Mice were divided into four groups (8–10 tumors per group): (*a*) 9L/pBabe tumors, untreated; (*b*) 9L/pBabe tumors, cyclophosphamide treated every 6 days; (*c*) 9L/2B6 tumors, cyclophosphamide treated every 6 days; and (*d*) 9L/2B11 tumors, cyclophosphamide treated every 6 days. Average tumor growth rates before cyclophosphamide treatment were similar in all four groups (average increases in tumor volume from days 14 to 23 after tumor implantation ranged from 3.8-fold to 5.6-fold). The effect of cyclophosphamide treatment on the growth rate of each tumor was calculated by comparison with the tumor volume on the day of the first cyclophosphamide injection (=100%) to facilitate comparisons of the effects of drug treatment on the growth of individual tumors that differ in size at the time of initial drug treatment.

Results

Retroviral Expression of P450 2B11 and P450R

9L cells were infected with retroviral particles encoding P450 2B11, transcribed as a bicistronic mRNA containing human P450R RNA linked via an IRES element. A pool of several thousand independent clones was obtained following puromycin selection, with each clone incorporating the P450-IRES-P450R cDNA at a random integration site and under the transcriptional control of the retroviral long terminal repeat promoter. 9L cell pools infected with a corresponding retrovirus coding for P450 2B1 or P450 2B6, IRES linked to P450R, were selected in parallel. P450 2B protein expression was readily detected by Western blot analysis of each 9L/P450 cell pool but not in 9L cells infected with the P450-deficient control retrovirus pBabe (Fig. 1A). Cellular P450 contents were 13, 27, and 16 pmol P450/mg total cell lysate for 9L/2B1, 9L/2B6, and 9L/2B11 cells, respectively. These P450 protein levels are similar to

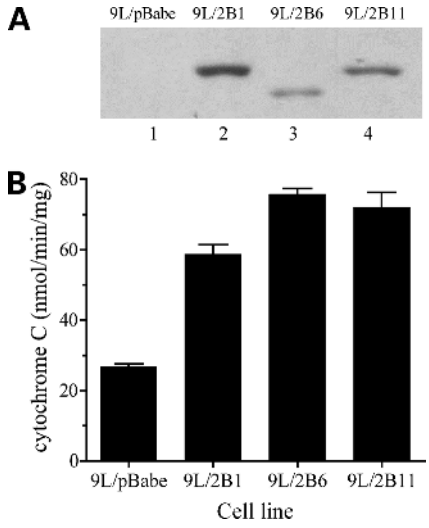

Figure 1. Retroviral expression of P450 2B proteins and P450R activity in 9L gliosarcoma cells. Rat 9L gliosarcoma cells were infected with retrovirus encoding P450 2B1, 2B6, or 2B11 in IRES linkage with P450R or with empty retrovirus (pBabe control) as described in Materials and Methods. Pools of puromycin-resistant cells were sonicated and analyzed for P450 protein by Western blotting using rabbit anti-P450 2B1 polyclonal antibody, which preferentially reacts with P450 2B1 and cross-reacts with P450s 2B6 and 2B11 (**A**). P450R enzyme activity (rate of cytochrome *c* reduction) was assayed using 20 μg cell lysate (**B**). *Columns,* mean (n = 2); *bars,* half the range. Samples in **A** are 9L control cell lysates (*lane 1*) and lysates of 9L cells expressing P450 2B1 (*lane 2*), 2B6 (*lane 3*), and 2B11 (*lane 4*); (50 μg protein/well).

those obtained previously by retroviral expression of P450 2B6 (18). P450R activity measured in the 9L/P450 cell lysates was increased up to 2.7-fold compared with 9L control cells (Fig. 1B), confirming the coexpression of P450 and the IRES-linked P450R cDNA.

Cytotoxicity of Cyclophosphamide and Ifosfamide toward 9L/P450 Cells

The P450-expressing 9L cells were sensitive to the cytotoxic effects of cyclophosphamide (Fig. 2A) and ifosfamide (Fig. 2B), whereas the P450-deficient 9L wild-type cells were insensitive to millimolar concentrations of both prodrugs. 9L/2B11 cells were the most susceptible to cyclophosphamide and ifosfamide cytotoxicity, with >90% growth inhibition observed at 50 μmol/L of each prodrug. The increased chemosensitivity of the 9L/2B11 cells was particularly striking at low concentrations of cyclophosphamide or ifosfamide (5–10 μmol/L), whereas the other 9L/P450 cells displayed little (9L/2B1 cells) or no growth inhibition (9L/2B6 cells), despite their similar levels of P450 and P450R expression. EC_{50}s determined for inhibition of 9L/2B11 cell growth by cyclophosphamide and ifosfamide (2.2–2.6 μmol/L) were 13- to 18-fold lower than for 9L/2B1 cells and 100- to 250-fold lower than for 9L/2B6 cells (Table 1).

P450 2B11 Is a High-Efficiency, Low K_m Catalyst of Cyclophosphamide and Ifosfamide 4-Hydroxylation in Intact 9L Cells

The striking sensitivity of 9L/2B11 cells to low micromolar prodrug concentrations may reflect the low K_m for cyclophosphamide and ifosfamide that *Escherichia coli*–expressed P450 2B11 exhibits *in vitro* (34). To test this hypothesis, we investigated whether the cellular cyclophosphamide and ifosfamide 4-hydroxylase activity of each cell line is related to its cyclophosphamide and ifosfamide cytotoxicity profile. In particular, we wanted to determine if the low K_m that bacterial-expressed P450 2B11 exhibits for cyclophosphamide and ifosfamide in a reconstituted enzyme system (34) is also manifest when the P450 is expressed in intact tumor cells. Figure 3 presents the concentration-dependent profiles for 4-hydroxylation of cyclophosphamide (Fig. 3A) and ifosfamide (Fig. 3B) catalyzed by each 9L/P450 cell line. Cyclophosphamide and ifosfamide metabolism catalyzed by 9L/2B11 cells was saturated at a substantially lower prodrug concentration than 9L/2B1 or 9L/2B6 cells. Steady-state kinetic analysis revealed a K_m of 70 μmol/L for cyclophosphamide 4-hydroxylation by 9L/2B11 cells (i.e., 7- and ~20-fold lower than the corresponding K_m exhibited by 9L/2B1 and

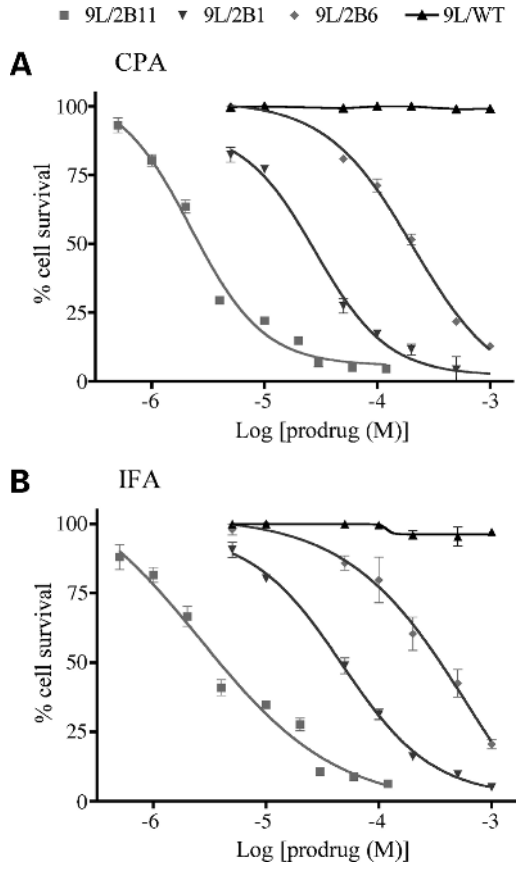

Figure 2. Growth inhibitory effect of cyclophosphamide (*CPA*; **A**) and ifosfamide (*IFA*; **B**) toward 9L/P450 cells. Cells seeded at 4,000 per well in 48-well plates were treated with increasing concentrations of cyclophosphamide or ifosfamide for 4 d. Growth inhibition assays were carried out with each of the indicated 9L/P450 and wild-type 9L cells. Cell growth in comparison with drug-free control samples was determined by crystal violet staining. *Points,* mean (n = 3 replicates); *bars,* SD. Error bars are too small to be seen for some of the data points. EC_{50}s calculated from these data are shown in Table 1.

Table 1. K_m, V_{max}, and EC_{50} for 9L/P450 cells incubated with cyclophosphamide and ifosfamide

	9L/2B1	9L/2B6	9L/2B11
Cyclophosphamide			
EC_{50}	28	207	2.2
K_m	490	1,380	70
V_{max}	18.4	24.1	35.0
V_{max}/K_m	37.5	17.5	500
Ifosfamide			
EC_{50}	47	652	2.6
K_m	810	1,460	35
V_{max}	6.4	1.6	5.9
V_{max}/K_m	7.9	1.1	168

NOTE: 9L cells expressing the indicated P450s in combination with P450R were assayed for cyclophosphamide and ifosfamide 4-hydroxylation as described in Fig. 3. V_{max} and K_m were then calculated as described in Materials and Methods. K_m and EC_{50} are in units of μmol/L, V_{max} are in units of nmol/4 hours/A_{595}, and V_{max}/K_m are in nmol/4 hours/A_{595}/mmol/L. EC_{50} are derived from the representative growth inhibition assays for each 9L/P450 cell line or 9L control cells shown in Fig. 2.

9L/2B6 cells, respectively; Table 1). 9L/2B11 cells also exhibited a higher V_{max} than 9L/2B1 and 9L/2B6 cells, resulting in a 13- to 29-fold higher overall catalytic efficiency (V_{max}/K_m). In the case of ifosfamide, the K_m of 9L/2B11 cells (35 μmol/L) was 23-fold lower than that of 9L/2B1 cells and 42-fold lower than 9L/2B6 cells. Overall, the increase in V_{max}/K_m for ifosfamide 4-hydroxylation by 9L/2B11 cells was 21- and 153-fold when compared with 9L/2B1 and 9L/2B6 cells, respectively (Table 1). These kinetic data are consistent with the cyclophosphamide and ifosfamide cytotoxicity profiles shown in Fig. 2.

Bystander Killing Effect

Tumor cell expression of P450 2B enzymes, and the associated activation of cyclophosphamide and ifosfamide, leads to formation of cell-permeable metabolites that exert bystander cytotoxicity toward P450-deficient neighboring tumor cells (8, 18). The high prodrug metabolic activity of 9L/2B11 cells indicates that these cells produce high intracellular concentrations of activated cyclophosphamide and ifosfamide, which could, in turn, lead to rapid death of the P450 2B11-expressing cells, thereby limiting the overall bystander cytotoxic response. We therefore investigated the ability of 9L/2B11 cells to induce a bystander cytotoxic response. Figure 4 shows that cyclophosphamide treatment of 9L/2B11 cells led to substantial bystander killing of cocultured wild-type 9L cells even when the P450-expressing cells represented only 10% of the total tumor cell population (Fig. 4C). By contrast, 9L/2B6 cells exhibited little or no bystander killing at low concentrations of cyclophosphamide and exhibited only a modest bystander effect at high cyclophosphamide concentrations (Fig. 4A). For example, at 20% 9L/2B11 cells, 100 μmol/L cyclophosphamide killed 86% of the total cell population, corresponding to at least 82% bystander killing (see Fig. 4). The corresponding bystander killing by 9L/2B6 cells was only 15% or ~5-fold lower. The bystander effect exerted by 9L/2B1 cells (Fig. 4B) was somewhat weaker than that of 9L/2B11 cells, killing 64% of the overall population when 9L/2B1 cells constituted 20% of the population. At low cyclophosphamide concentrations (10 μmol/L), 49% of bystander cells were killed when the population was seeded with 20% 9L/2B11 cells, whereas only 12% bystander killing was effected by 9L/2B1 cells under the same conditions. Further studies focused on the comparison of CYP2B11 with CYP2B6, which has recently been entered into clinical trials in patients with advanced breast cancer and melanoma (29).

Adeno-2B11, a Replication-Defective Adenovirus Expressing P450 2B11 and P450R

A replication-defective adenovirus containing a P450 2B11-IRES-P450R expression cassette was engineered and designated Adeno-2B11. This adenovirus has the same design as Adeno-2B6 (26), which expresses P450 2B6 linked to P450R via an IRES sequence. Adeno-2B11 and Adeno-2B6

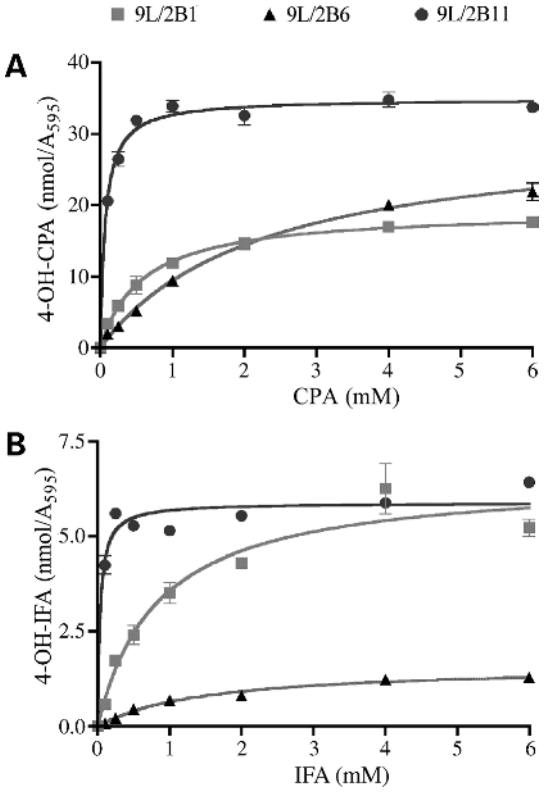

Figure 3. 4-Hydroxylation of cyclophosphamide and ifosfamide by 9L/2B1, 9L/2B6, and 9L/2B11 cells. Cells expressing the indicated P450s in combination with P450R were cultured at 10^5 per well of a 12-well plate and incubated for 4 h with cyclophosphamide (**A**) or ifosfamide (**B**) in the presence of 5 mmol/L semicarbazide followed by protein precipitation, metabolite derivatization, and HPLC analysis. Data are rates of metabolite production over the 4-h incubation period, expressed as nmol 4-OH metabolite per 2 mL culture medium per well, normalized for the cell density of each culture well (A_{595}; crystal violet staining intensity). *Points,* mean (duplicate determinations); *bars,* half the range. 4-Hydroxymetabolite production by 9L control cells was below the limit of detection. K_m and V_{max} for 4-hydroxylation of each prodrug substrate were determined by Eadie-Hofstee analysis of these and other data sets from two to three independent sets of determinations and are shown in Table 1. *Points,* mean; *bars,* half the range.

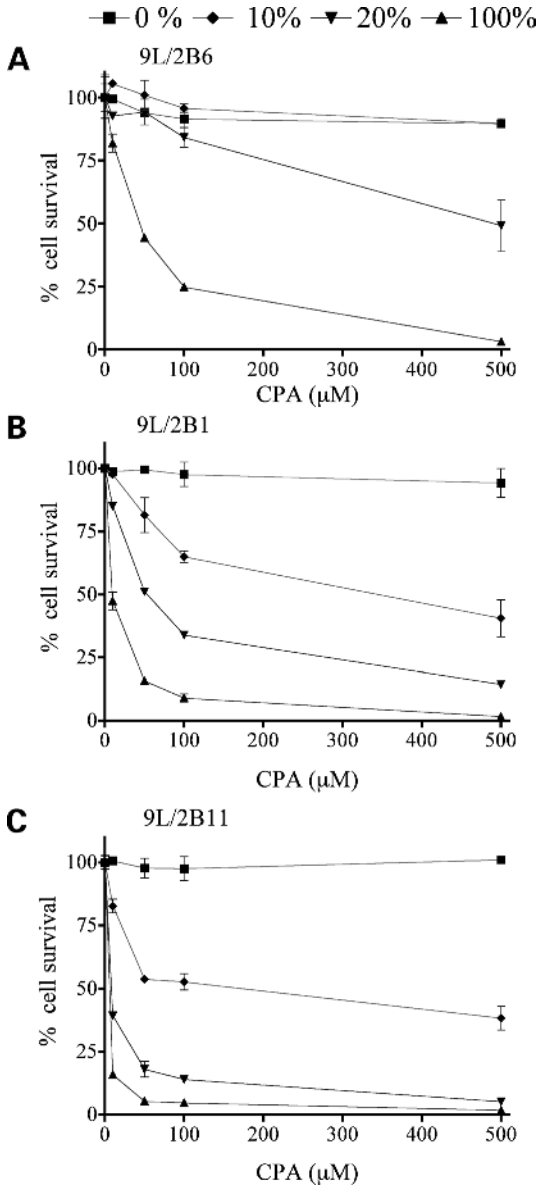

Figure 4. Bystander activity of 9L/2B6 and 9L/2B11 cells. Wild-type 9L cells were mixed with increasing percentages of 9L/2B6 cells (**A**), 9L/2B1 cells (**B**), or 9L/2B11 cells (**C**) (0%, 10%, 20%, and 100% 9L/2B cells) and seeded in 1 mL culture medium to give a total of 10^5 per well of a 12-well plate. Twenty hours later, the cells were changed to fresh medium containing cyclophosphamide for a period of 48 h. The culture medium was then replaced with fresh cyclophosphamide-containing medium and the cells were incubated for an additional 48 h. Cells remaining at the end of the 4-d cyclophosphamide treatment period were stained and quantified by crystal violet staining. Data are percent growth rate relative to the drug-free controls. *Points,* mean (n = 2 replicates from a typical experiment); *bars,* SD. The extent of bystander killing was determined as shown by the following example. At 100 μmol/L cyclophosphamide and at 20% 9L/2B11 cells, 14% cell survival (86% cell kill) was observed. This corresponds to 86% bystander cell killing if the 9L/2B11 cells and the 9L wild-type cells are equally sensitive to 4-OH-cyclophosphamide cytotoxicity. However, if the 20% population of 9L/2B11 cells are preferentially killed, then the bystander killing corresponds to 86% (total cell kill) − 20% (9L/2B11 cells killed in the population) = 66% bystander cell kill. Because the bystander cells constituted 80% of the original cell population, the fraction of bystander cells killed is 66% of the 80% 9L population or ~82%.

were compared with respect to their ability to induce P450R expression and cyclophosphamide activation in the human brain tumor cell line U251, assayed 48 hours after initiation of virus infection, at which time Adeno-2B6-dependent P450 expression is maximal (26). Both viruses induced dose-dependent increases in P450R activity, with a somewhat higher increase seen in cells infected with Adeno-2B6 compared with Adeno-2B11 (7-fold versus ~5-fold increase at MOI 100; Fig. 5A). By contrast, there was substantially greater conversion of cyclophosphamide (100 μmol/L) to 4-OH-cyclophosphamide by cells infected with Adeno-2B11 compared with Adeno-2B6 (5.5 versus 0.2 μmol/L 4-OH-cyclophosphamide released into culture medium; Fig. 5B).

Adeno-2B6 and Adeno-2B11 both effected dose-dependent increases in cyclophosphamide toxicity toward U251 cells. However, the overall cytotoxic response was substantially greater with Adeno-2B11 and could be achieved at a much lower prodrug concentrations (Fig. 5D versus Fig. 5C), consistent with the metabolic data shown in Fig. 5B. For example, U251 cells infected with 50 MOI Adeno-2B6 showed moderate cyclophosphamide cytotoxicity (25% cell kill) at 50 μmol/L cyclophosphamide, whereas ~85% cell killing was achieved with Adeno-2B11 under comparable conditions. The superiority of Adeno-2B11 was most apparent at 10 to 20 μmol/L cyclophosphamide, consistent with the low K_m (cyclophosphamide) of P450 2B11. The strong cytotoxicity conferred by Adeno-2B11 was associated with substantial bystander killing of the uninfected U251 cells in the population. Thus, although only 10 ± 2.5% of the U251 cells expressed P450 2B11 as shown by immunostaining of cells infected with MOI 25 Adeno-2B11 (Fig. 6B versus Fig. 6A), major cytotoxicity was still seen following treatment with 20 μmol/L cyclophosphamide, with the results most dramatic after a 7-day treatment period (Fig. 6C and D).

Effect of Onyx-017 on Adeno-2B11-Dependent Cyclophosphamide Cytotoxicity

Onyx-017 is an E1b-55-kDa gene-deleted adenovirus that harbors a wild-type E3 region, which contains a myriad of genes involved in cell death and other adenoviral processes (45). E1b-55-kDa functions include p53 degradation, RNA export, and host protein shutoff, and the loss of these E1b-55-kDa late functions is an important determinant of the tumor cell selectivity of the Onyx virus (46). Onyx-017 can also serve as a helper virus that facilitates intratumoral replication and cell-to-cell spread of replication-defective adenovirus, such as Adeno-2B6 (26). Given the extraordinary ability of P450 2B11 to activate cyclophosphamide at low prodrug concentrations, we investigated the effect of Adeno-2B11 + Onyx-017 on cyclophosphamide cytotoxicity. These experiments were carried out in U251 tumor cells, which are permissive to adenovirus infection, and PC-3 tumor cells, which are relatively resistant to infection (26).

Cells were infected with Adeno-2B11 or Adeno-2B6 at MOI 8 (U251 cells) or MOI 32 (PC-3 cells) either alone or in combination with Onyx-017. The higher adeno-P450 MOI was used for the PC-3 cells to compensate for the low adenovirus infectivity of this cell line. Substantial increases

in cyclophosphamide cytotoxicity were seen in tumor cells infected with Adeno-2B11 + Onyx-017 compared with Adeno-2B6 + Onyx-017 (Fig. 7). For example, Adeno-2B11 combined with Onyx-017 (MOI 2) induced an 88% decrease in U251 cell survival at 50 μmol/L cyclophosphamide (Fig. 7B), whereas Adeno-2B6 + Onyx-017 effected <20% cell killing under comparable conditions (Fig. 6A). At higher MOIs, Onyx-017 further increased the cytotoxicity of low cyclophosphamide concentrations toward the Adeno-2B11-infected U251 cells. In the prostate carcinoma cell line PC-3, no cyclophosphamide-dependent cytotoxicity was seen with either adeno-P450 virus alone, owing to the very poor infectivity of these cells. Coinfection with Onyx-017 sensitized the cells to cyclophosphamide, with the effects being much more dramatic in the case of Adeno-2B11, particularly at low cyclophosphamide concentrations (Fig. 7D versus Fig. 7C).

By coamplifying the replication-defective Adeno-2B6 and spreading it to neighboring tumor cells, Onyx-017 can dramatically increase overall P450 metabolic activity (26). This spreading effect of Onyx-017 was also seen with Adeno-2B11 as shown by the ability of culture medium from Adeno-2B11 + Onyx-017 coinfected U251 cells, but not culture medium from cells infected with Adeno-2B11 alone, to deliver P450 2B11 to fresh U251 cells (data not shown). The extent to which Onyx-017 coamplifies Adeno-2B11 could be quantified by measuring P450 2B11 RNA levels in U251 cells infected either with Adeno-2B11 alone or with Adeno-2B11 + Onyx-017. Dramatic increases in P450 2B11 RNA as well as adenovirus E3 RNA were seen in the coinfected cells, showing the helper effect of Onyx-017 on Adeno-2B11 transgene expression (Table 2). Similar increases in P450 2B6 RNA were seen in Adeno-2B6 + Onyx-017 coinfected cells (data not shown). Furthermore, evaluation of P450 metabolic activity revealed substantially higher 4-OH-cyclophosphamide formation in cyclophosphamide-treated U251 cells infected with Adeno-2B11 + Onyx-017 compared with adeno-P450 2B6 + Onyx-017 (Fig. 7E) despite similar increases in P450R activity induced by Adeno-2B6 and Adeno-2B11 (data not shown). Thus,

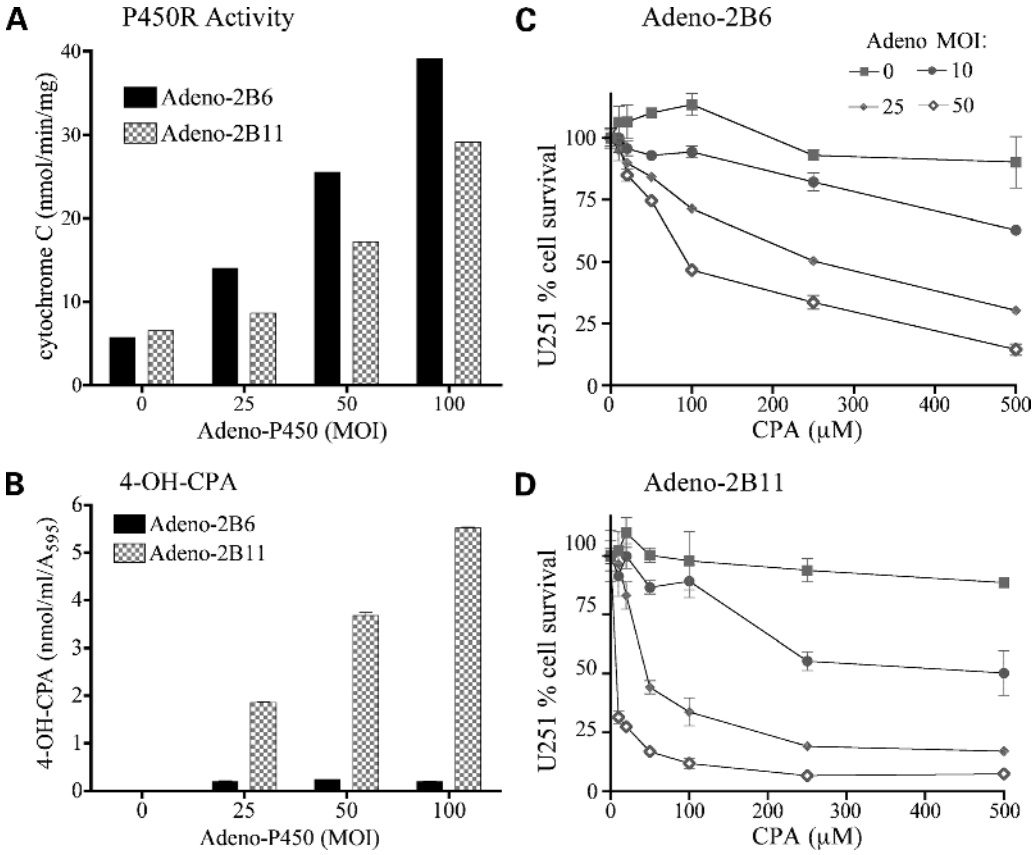

Figure 5. P450R expression and cyclophosphamide 4-hydroxylase activity in U251 cells infected with adeno-P450. U251 cells were seeded in six-well plates at 10^5 per well. Sixteen hours later, the cells were infected with Adeno-2B6 or Adeno-2B11 overnight at the indicated MOIs. **A,** adenovirus-infected cells were incubated for an additional 24 h followed by assay of P450R activity (cytochrome *c* reduction) to obtain an overall indication of viral transduction efficiency. **B,** virus-infected cells were treated for 4 h with 100 μmol/L cyclophosphamide in 3 mL fresh RPMI 1640 containing 5% FBS and 5 mmol/L semicarbazide to stabilize the 4-OH-cyclophosphamide metabolite. Duplicate aliquots of culture medium were removed and assayed for 4-OH-cyclophosphamide by HPLC. Data are normalized to the cell density of each sample (A_{595} following crystal violet staining). **C** and **D,** U251 cells seeded in 24-well plates at 14,000 per well were infected for 24 h with Adeno-2B6 (**C**) or Adeno-2B11 (**D**) at MOI 0, 10, 25, or 50. The cells were then treated with cyclophosphamide as described in Materials and Methods. Cells were then stained with crystal violet and quantified (A_{595}) as percentage cell survival relative to drug-free controls.

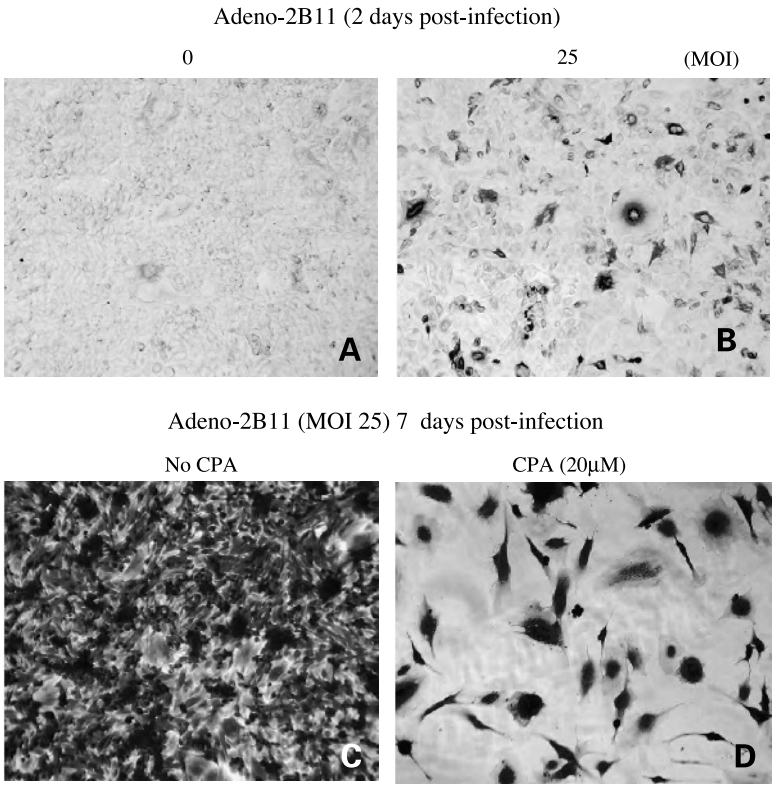

Figure 6. Visualization of Adeno-2B11-infected U251 cells conferring bystander cyclophosphamide killing. U251 cells were infected with Adeno-2B11 at MOI 0 (**A**) and MOI 25 (**B**) and stained with anti-CYP2B11 antibody 2 d postinfection. Cell counting indicated the presence of 10 ± 2.5% CYP2B11 stained cells in the overall U251 cell population (**B**). Parallel plates of Adeno-2B11-infected cells were treated without cyclophosphamide (**C**) or with 20 μmol/L cyclophosphamide (**D**) for 7 d and then stained with crystal violet to determine U251 cell survival.

although the helper effect of Onyx-017 on the replication and spread of Adeno-2B11 and Adeno-2B6 is fundamentally the same, the superior metabolic activity of Adeno-2B11 results in much greater increases in tumor cell production of 4-OH-cyclophosphamide.

Adeno-P450-Enhanced Cyclophosphamide Activity in Drug-Resistant MCF-7 Cells

We next investigated the ability of Adeno-2B11 to kill MCF-7 breast cancer cells resistant to activated cyclophosphamide (MCF-7/4HC cells). A ~5-fold higher MOI of adeno-P450 was used to infect the MCF-7/4HC cells in an effort to overcome the 6-fold drug resistance of this cell line (36). Figure 8A shows that the drug-sensitive parental MCF-7 cell line was sensitized to cyclophosphamide by Adeno-2B11 + Onyx-017 coinfection to a greater extent than by Adeno-2B6 + Onyx-017 coinfection. Onyx-017 (MOI 3) exerted little or no intrinsic cytotoxicity under these conditions, and Adeno-2B11 exhibited only moderate toxicity in the absence of Onyx-017. These treatments were much less toxic toward MCF-7/4HC cells as anticipated. Nevertheless, Adeno-2B11, but not Adeno-2B6, was able to induce cyclophosphamide-dependent killing of MCF-7/4HC cells when coinfected with Onyx-017 (Fig. 8B). Thus, the high metabolic activity of Adeno-2B11 can, in part, help overcome acquired resistance to activated cyclophosphamide.

Effect of P450 2B11 on Cyclophosphamide Antitumor Activity *In vivo*

9L tumor cells transduced with retrovirus encoding P450 2B11 or P450 2B6 and coexpressing P450R were grown as solid, s.c. tumors in *scid* mice. P450-deficient 9L tumors were studied in parallel as a control. Cyclophosphamide was given on an antiangiogenic (metronomic) schedule consisting of 140 mg cyclophosphamide/kg body weight i.p. repeated every 6 days (23) for up to 11 cyclophosphamide injections (22). This cyclophosphamide dose and schedule is accompanied by minimal host toxicity (22, 23) and contrasts to a maximally tolerated dose of 265 mg cyclophosphamide/kg body weight given as a single injection in the same *scid* mouse model (47).

Untreated 9L tumors grew rapidly, necessitating that the animals be killed by day 49 post-tumor implantation (day 26 on the *X axis* in Fig. 9A). All of the 9L control and 9L/P450 tumors responded to 6-day repeated cyclophosphamide treatment as indicated by the substantial decreases in volume of each individual tumor (Fig. 9B–D). Tumor growth was arrested after the third cyclophosphamide injection (days 12–15 posttreatment) in the case of the 9L/2B6 and 9L/2B11 tumors. This was followed by major regression leading to an apparent elimination of all 10 of the P450 2B11-expressing tumors by the 7th cyclophosphamide injection (days 35–39 posttreatment; Fig. 9D). By contrast, only 3 of 10 tumors that expressed P450 2B6 were eliminated by day 43, and it was not until day 57 (after the 10th cyclophosphamide injection) that the 9L/2B6 tumors regressed to the point where they were no longer measurable. Control 9L tumors given the cyclophosphamide 6-day treatment regressed by an average of only 83% in contrast to the complete regression seen with 9L/2B6 and 9L/2B11 tumors (Table 3).

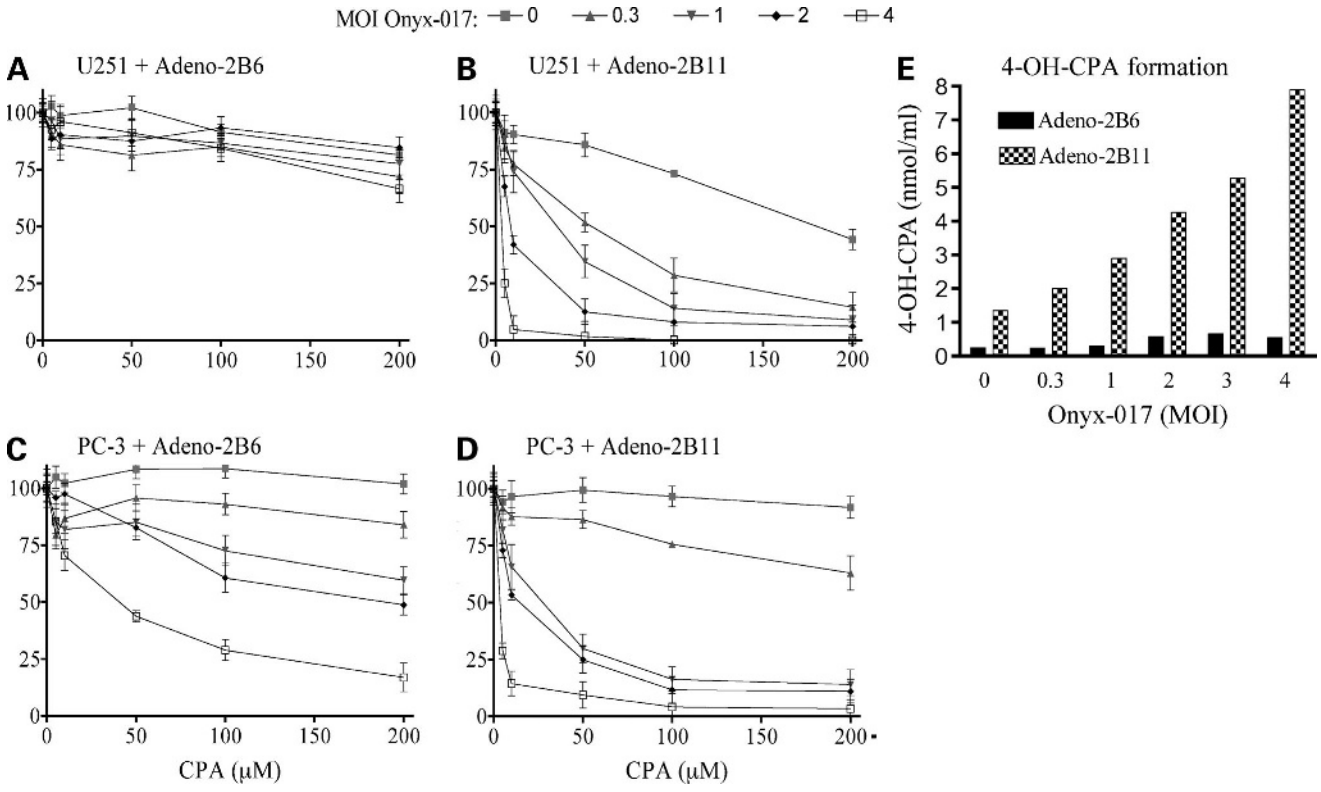

Figure 7. Effect of Onyx-017 on cyclophosphamide 4-hydroxylation and cytotoxicity in U251 and PC-3 cells infected with Adeno-2B6 or Adeno-2B11. **A–D,** U251 and PC-3 cells seeded in 24-well plates of 14,000 per well were infected for 24 h with adeno-P450 (MOI 8 for U251 and MOI 32 for PC-3) alone or in combination with Onyx-017 (MOI 0–4). Cells were then treated with 0 to 1,000 μmol/L cyclophosphamide in 1 mL fresh RPMI 1640 containing 5% FBS for a total of 6 d followed by crystal violet staining. Data are percent growth rate relative to the drug-free controls. *Points,* mean ($n = 2$ replicates from a typical experiment); *bars,* SD. **E,** U251 cells were infected for 24 h with Adeno-2B6 or Adeno-2B11 (MOI 12) alone or in combination with Onyx-017 (MOI 0–4). Cells were then cultured for an additional 24 h, at which point the culture medium was replaced with fresh medium containing cyclophosphamide (250 μmol/L) and 5 mmol/L semicarbazide for a 4-h period. The formation of 4-OH-cyclophosphamide was determined by HPLC. The intrinsic toxicity of Onyx-017 in the absence of cyclophosphamide was negligible in PC-3 cells (MOI 0–3) with a slight toxicity at MOI 4 (~8.5% PC-3 cell death). U251 cells were more sensitive to Onyx-017 toxicity (~13–25% cell death at MOI 0.3 and 3, respectively), with a more pronounced toxicity observed at Onyx-017 MOI 4 (40–45% cell death; data not shown).

The much greater responsiveness of both 9L/P450 tumor types was also apparent from the period of continued tumor growth that immediately followed initiation of the 6-day cyclophosphamide treatment schedule (Table 3). Thus, the P450-deficient tumors continued to increase in volume by an average of 450% before they began to regress, whereas the P450 2B6 and P450 2B11 tumors increased by an average of only 250% to 280% and then began to regress.

Cyclophosphamide treatment was halted after the 11th cyclophosphamide injection (day 60) to ascertain whether any viable tumor cells remained. The P450-deficient 9L control tumors resumed aggressive growth beginning ~18 days after cyclophosphamide treatment was discontinued (Fig. 9B). By contrast, the P450 2B6-transduced tumors exhibited an average tumor-free period of 30 days (range, 21–39 days), after which they resumed growth. The 9L/2B11 tumors, however, had a substantially longer tumor-free period (mean, 79 days; range, 60–100), and only 2 of the 10 tumors exhibited aggressive regrowth when the experiment was terminated on day 134 (Fig. 9D; Table 3).

Discussion

P450 prodrug gene therapy has several unique characteristics that distinguish it from other cancer GDEPT strategies. One important feature is its provision of two distinct routes for prodrug activation, a hepatic route and an intratumoral route (primary tumor and its metastases), which results in the tumor being exposed to activated metabolites from both an extratumoral (systemic) compartment and a local, intratumoral compartment. Other GDEPT strategies use prodrugs that are not metabolized in the liver, limiting therapeutic activity to cells nearby those cells infected with the prodrug-activating gene therapy vector. Moreover, liver-activated P450 prodrugs, such as cyclophosphamide, exert both a systemic antitumor bystander effect and a powerful cytotoxic effect directed against tumor-associated endothelial cells (antiangiogenic activity). This latter effect is manifest when cyclophosphamide is given using a metronomic schedule (23) and greatly enhances the regression of tumors that coexpress P450 2B6 and P450R (22). However, a key limitation of P450-based

gene therapy is the high K_m that characterizes most mammalian P450 enzymes with their drug substrates (e.g., K_m, 500–2,000 μmol/L for cyclophosphamide and ifosfamide with P450 2B1 and P450 2B6; refs. 30, 31). This leads to inefficient prodrug activation at pharmacologically relevant drug concentrations (e.g., ~50–200 μmol/L cyclophosphamide and ifosfamide; refs. 32, 33). The goal of the present study, therefore, was to investigate whether P450 GDEPT can be enhanced using P450 2B11, a canine P450 enzyme that was recently identified as a low K_m catalyst of cyclophosphamide and ifosfamide activation (34) and displays kinetic properties far superior to those of P450 enzymes 2B1 and 2B6, used previously in preclinical and clinical GDEPT studies.

We first investigated the chemosensitization of 9L gliosarcoma cells to cyclophosphamide and ifosfamide following infection with retrovirus that delivered P450 2B1, 2B6, or 2B11 at similar expression levels. Each P450 was delivered in combination with P450R, which catalyzes the rate-limiting electron transfer step required for all microsomal P450 drug oxidations and can markedly improve P450 metabolic activity and antitumor responses when introduced into tumor cells in combination with P450 (18, 19). The resultant pool of 9L/2B11 cells was highly sensitive to low micromolar concentrations of cyclophosphamide and ifosfamide (EC_{50}, 2.2–2.6 μmol/L) in contrast to the corresponding 9L/2B1 and 9L/2B6 cell pools, which required up to 100- to 250-fold higher prodrug concentrations for effective cell killing. The enhanced chemosensitivity of 9L/2B11 cells was associated with correspondingly higher cyclophosphamide and ifosfamide 4-hydroxylation (prodrug activation) and K_m values for prodrug metabolism measured in intact cells (K_m, 35–70 μmol/L) that were 20- to 40-fold lower than 9L/2B6 cells (K_m, 1,380–1,460 μmol/L; Table 1). Although P450 2B11 exhibits 22% to 26% amino acid difference from P450s 2B1 and 2B6, its unique kinetic properties are most likely due to a limited number of amino acid substitutions at the active site. These include a valine residue at position 114, which when introduced into P450 2B1 decreases the K_m toward cyclophosphamide and ifosfamide up to 4-fold (34). The presence of this and other naturally occurring ''mutations'' in P450 2B11 gives rise to a 29- to 153-fold higher overall catalytic efficiency (V_{max}/K_m) for cyclophosphamide and ifosfamide 4-hydroxylation, with corresponding increases in cyclophosphamide cytotoxicity, in tumor cells that express P450 2B11 compared with P450 2B6.

Studies using Adeno-2B11, a replication-defective adenovirus delivering P450 2B11 in combination with P450R,

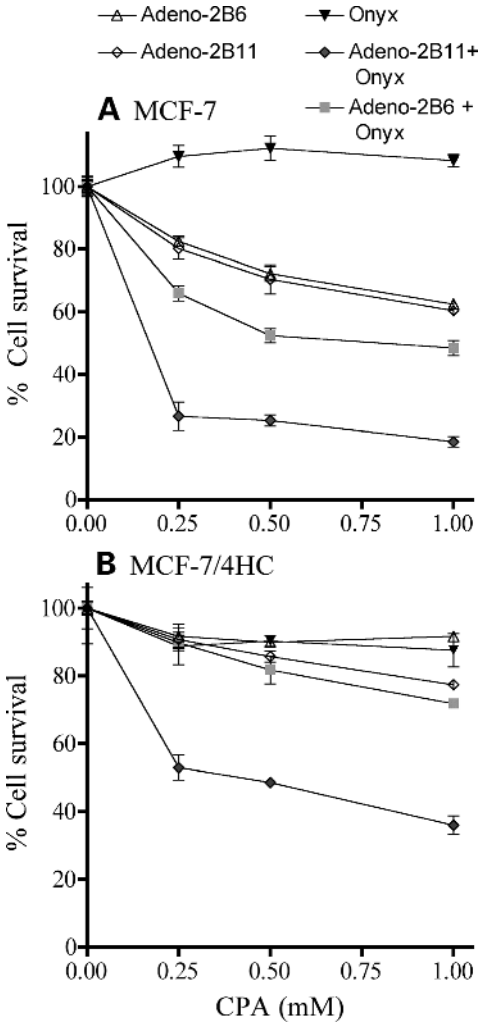

Figure 8. Effect of adeno-P450 on cytotoxicity of cyclophosphamide toward MCF-7 cells (**A**) and MCF-7/4HC cells (**B**). Cells were infected with Adeno-2B6 or Adeno-2B11 (MOI 32 for MCF-7/4HC and MOI 6 for MCF-7 cells) with or without Onyx-017 (MOI 3) and then treated with cyclophosphamide for a total of 6 d as in Fig. 7. Cells remaining at the end of the experiment were quantified by crystal violet staining. Data are percent cell survival relative to the drug-free controls. *Points,* mean (n = 2 replicates for a representative experiment); *bars,* SD. The intrinsic toxicity of Onyx-017 toward MCF-7 cells was reflected in the death of ~24% of MCF-7 cells and ~17% of MCF-7/4HC cells at Onyx-017 MOI 3 in the absence of cyclophosphamide (data not shown).

Table 2. Onyx-017-enhanced expression of adeno-2B11

	P450 2B11 RNA	E3 RNA
No virus	1	1
Adeno-2B11	145 ± 75	1 ± 0.7
Adeno-2B11 + Onyx-017 (MOI 1)	2,350 ± 165	9,550 ± 2,000
Adeno-2B11 + Onyx-017 (MOI 2)	3,600 ± 500	20,900 ± 3,300
Adeno-2B11 + Onyx-017 (MOI 4)	6,200 ± 1,000	49,500 ± 7,400

NOTE: U251 cells (1×10^5) seeded in six-well plates were infected with adeno-2B11 (MOI 8) alone or in combination with Onyx-017 (MOI 1, 2, or 4 as indicated) in a volume of 1 mL for 4 hours followed by the addition of 2 mL culture medium for an additional 20 hours (total virus infection, 24 hours). The medium was then changed and the cells were incubated for an additional 24 hours. Cells were collected and lysed using TRIzol reagent according to the manufacturer's instructions for cell monolayers. Reverse transcription to yield cDNA followed by quantitative real-time PCR was carried out as described in Materials and Methods. P450 2B11 and E3 RNA were both induced to similar levels (C_T, 19.3–19.7 for both); the larger fold induction that is apparent for E3 reflects the much lower basal level of its RNA in uninfected control cells compared with P450 2B11 RNA (data not shown).

further established the superior activity of this enzyme combination for P450 GDEPT using cyclophosphamide. The increased activity of P450 2B11 compared with P450 2B6 was manifest in human tumor cell lines readily infected by adenovirus (U251 cells) and in cells with a lower intrinsic susceptibility to adenovirus infection (PC-3 and MCF-7 cells). P450 expression and cyclophosphamide-dependent cell killing could be greatly enhanced by coinfection with the conditionally replicating, oncolytic adenovirus Onyx-017. Enhanced cyclophosphamide-dependent cell killing was also seen in an MCF-7 cell line resistant to activated cyclophosphamide (MCF-7/4HC cells), showing the potential of P450 GDEPT to extend the effectiveness of cyclophosphamide therapy to include drug-resistant tumor cells. Further increases in activity against tumor cells showing intrinsic or acquired drug resistance to P450 prodrugs may be achieved by directed P450 evolution (48) or through further optimization of the gene delivery vector to increase intratumoral P450 expression and P450 metabolic activity.

The use of a low K_m P450 enzyme, such as P450 2B11, could be particularly useful for GDEPT applications in certain patient populations, such as children with B-cell non-Hodgkin's lymphoma, where inadequate (hepatic) conversion of cyclophosphamide to active metabolites is associated with an increased risk of disease recurrence (49). Consequently, for patients with low rates of cyclophosphamide clearance and for individuals who produce significant quantities of inactive cyclophosphamide metabolites (49), P450 gene therapy may well prove to be clinically beneficial. This approach may be more effective than increasing the dose of cyclophosphamide, which can lead

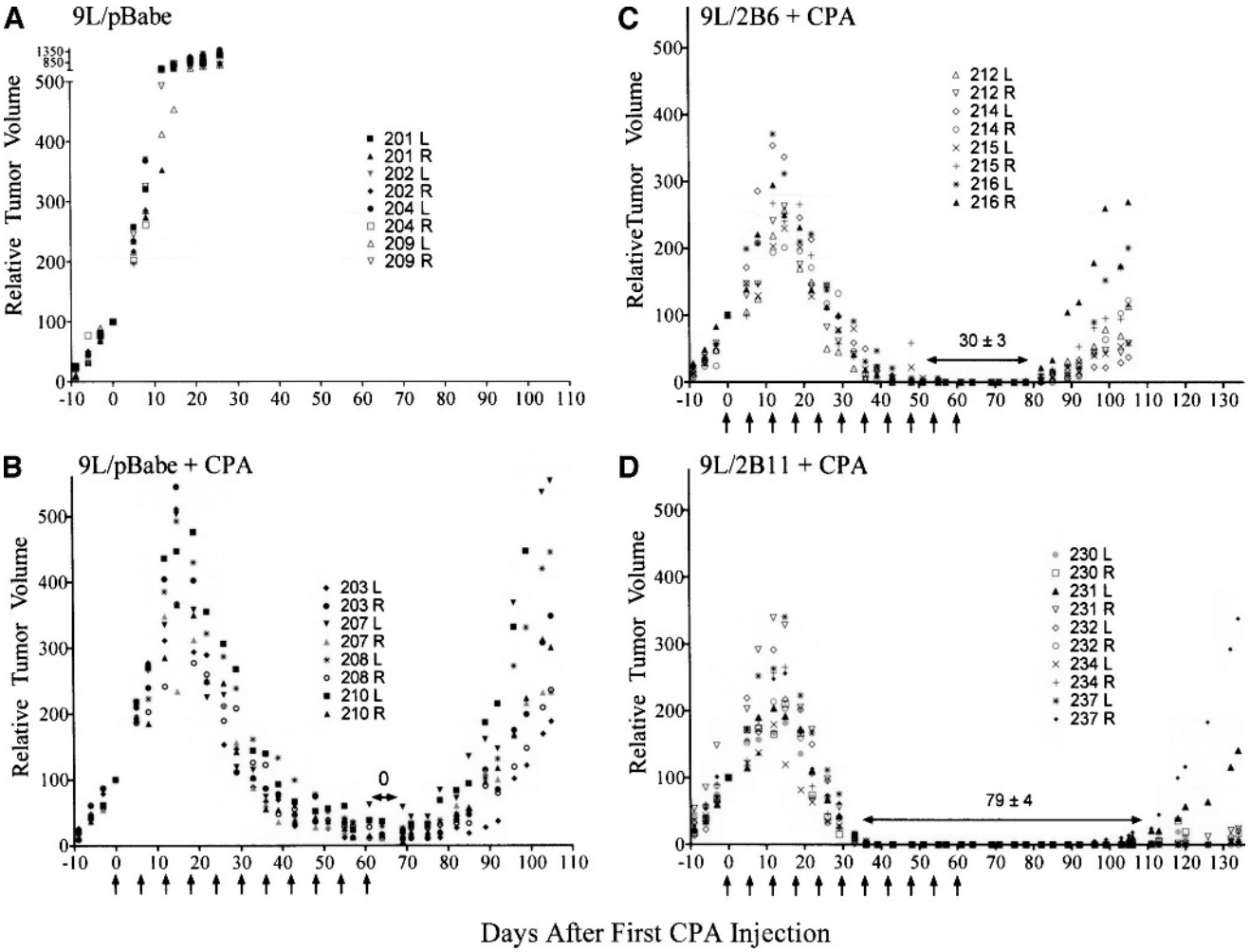

Figure 9. Effect of P450 2B11 expression on cyclophosphamide-induced tumor growth delay. 9L control tumors (9L/pBabe; **A** and **B**), 9L/2B6 tumors (**C**), and 9L/2B11 tumors (**D**) were implanted s.c. on each flank of *scid* mice. Tumor areas were measured twice weekly with a caliper and tumor volumes were calculated as described in Materials and Methods. Mice were untreated (**A**) or were treated with a series of 11 cyclophosphamide injections at 140 mg/kg body weight i.p. spaced 6 d apart (*X axis*, *arrows*). Data are based on volumes of individual tumors, shown as a percentage of the tumor volume on day 0 (first cyclophosphamide treatment; $n = 8-10$ tumors per treatment group). Cyclophosphamide treatment began on day 23 after tumor implantation (*Y axis*, *day 0*; i.e., when the average tumor volume reached ~1,000–1,200 mm^3; Table 3). Cyclophosphamide-induced tumor regression led to a tumor-free period defined as the time period (in days) when tumors were not palpable (**B**–**D**, *double-headed arrow*).

Table 3. Effect of cyclophosphamide 6-day treatment schedule on growth of 9L and 9L/P450 tumors

	Initial response to cyclophosphamide			Cyclophosphamide injections required for full tumor regression	Maximal tumor regression (%)*	Tumor-free period (d)†
	Initial tumor volume (mm^3)‡	Continued tumor growth period (d)§	Tumor size increase (%)‖			
9L	1,134 ± 82 (8)	26 (Killed)	1,159 ± 131	¶	0	0
9L + cyclophosphamide/6 d	1,060 ± 93 (8)	15–19 (16 ± 0.7)	446 ± 30	**	83 ± 4	0
9L/2B6 + cyclophosphamide/6 d	984 ± 62 (8)	12–15 (13.5 ± 0.6)	280 ± 21	10–11	100	30 ± 3 (21–39)
9L/2B11 + cyclophosphamide/6 d	1,246 ± 72 (10)	12–15 (13.5 ± 0.5)	248 ± 19	7–8	100	79 ± 4 (60–100)

*Maximal decrease in tumor size, which generally was achieved after 7 to 11 cyclophosphamide injections. Percentage regression values were calculated based on the volume of each tumor at the time of first cyclophosphamide injection (cf., column 1; mean ± SE).

†Length of tumor-free periods before growth resumed after cessation of cyclophosphamide treatment. Data are expressed as mean ± SE (days). Values in parentheses are range (in days) for individual tumors in each group. One 9L/2B11 tumor was still not palpable when the experiment was terminated on day 134.

‡Tumor volume at time of first cyclophosphamide injection, mean ± SE for (n) individual tumors, calculated from measured tumor areas.

§Time, measured in days after first cyclophosphamide injection, until tumor regression was first detected in tumor size measurements taken twice weekly. Data are expressed as a range exhibited by the individual tumors in each group. Untreated 9L tumor controls did not regress; mice were killed 26 days after initiation of cyclophosphamide treatment of the other groups.

‖Percentage increase in tumor size from time of first cyclophosphamide injection until mice were killed (untreated 9L controls) or tumor regression was first observed (cyclophosphamide-treated tumors; mean ± SE).

¶Not applicable.

**Full tumor progression was not achieved.

to saturation of the bioactivation pathway (50) and increased host toxicity. Other benefits of using P450 2B11, a canine enzyme, for P450 GDEPT include the potential for eliciting an antitumor immune response, leading to a systemic bystander effect that greatly increases the overall antitumor response. Indications of such an immunologic response were reported in a recent phase I trial of P450 GDEPT combined with low-dose cyclophosphamide in breast cancer patients (29). It should be noted, however, that such immune responses might negatively affect viral replication by increasing the elimination of vector-infected cells.

The bystander cytotoxic effect is critical to the success of any prodrug activation gene therapy strategy (51). One potential concern of using a highly active catalyst of cyclophosphamide activation, like P450 2B11, is that it may generate a high intracellular concentration of active drug, which in turn may accelerate death of the P450-expressing tumor cells, thereby limiting bystander cytotoxicity (52). Our studies showed, however, that 9L/2B11 cells mediate substantial bystander cytotoxicity, killing ~70% to 75% of bystander tumor cells under conditions where cyclophosphamide-treated 9L/2B6 cells killed only up to 15% of bystander tumor cells. Similarly, in a population of U251 cells infected with Adeno-2B11 under conditions where only ~10% of the cells express P450, >90% cell killing was observed at low-dose (20 μmol/L) cyclophosphamide. Further increases in bystander killing may be obtained by coexpression of the pan-caspase inhibitor p35 (53) or by introduction of other antiapoptotic factors that delay but do not abrogate cyclophosphamide-induced cell death (52).

The therapeutic potential of P450 2B11 was evaluated *in vivo* in *scid* mice in a tumor xenograft model. 9L tumors expressing a P450 2B11-IRES-P450R expression cassette fully regressed by day 39 of cyclophosphamide treatment compared with a 57-day cyclophosphamide treatment period required for comparable regression of 9L/2B6 tumors. Moreover, an extended tumor-free period was seen following cessation of cyclophosphamide treatment in the case of the 9L/2B11 tumors (up to 100 days) versus 9L/2B6 tumors (21–39 days). These findings highlight the advantages of using P450 2B11 to effect prodrug activation, particularly under conditions where intratumoral prodrug levels may be low (e.g., as a consequence of the reduced access that tumor cells may have to circulating cyclophosphamide as they regress in response to the antiangiogenic action of the 6-day repeating cyclophosphamide treatment schedule). In the case of 9L control tumors, cyclophosphamide effected delayed tumor regression as was seen previously (22). This can, in part, be attributed to apoptosis of the endothelial cells lining the tumor vasculature by liver-derived 4-OH-cyclophosphamide (23). Overall, the dramatic regression of both 9L/2B11 and 9L/2B6 tumors indicates a direct tumor cytotoxic action associated with intratumoral cyclophosphamide activation in addition to the endothelial cell-directed, antiangiogenic mechanism that is associated with liver cyclophosphamide activation, which may apply equally well to 9L control and 9L/P450 tumors.

The response of 9L/2B6 tumors to the metronomic, 6-day cyclophosphamide treatment schedule seen in the present study was less dramatic than that seen in a previous study, where cyclophosphamide had a more immediate inhibitory

effect on tumor growth (22). Moreover, the initial response of 9L/2B11 tumors in the present study was not apparently different from that of 9L/2B6 tumors. One possible explanation could be that, in the present study, the 9L/P450 tumors were derived from pools of retrovirus-infected 9L cells, each composed of several thousand independent clones. Each clone may express the P450, and P450R, with a markedly different efficiency, depending on where in the genome the retroviral sequence is inserted, and as a consequence, each clone may respond to cyclophosphamide in an idiosyncratic manner. In contrast, the 9L/2B6 tumors studied earlier were derived from a unique high P450 activity clone selected for high P450 2B6 expression (22). Consequently, all of the 9L/2B6 tumor cells responded to cyclophosphamide rapidly and in a similar manner. This conclusion is supported by immunohistochemical analysis of the present 9L/2B6 and 9L/2B11 tumors, which revealed substantial heterogeneity with respect to P450 expression at the time of initial cyclophosphamide treatment, with many of the tumor cells expressing little or no detectable P450 2B protein.[2] This finding is consistent with our use of pools of retrovirus-infected 9L cells and provides indirect evidence for an *in vivo* bystander effect in our tumor xenograft model. The present *in vivo* studies used established P450-expressing tumor cell lines to compare the effectiveness of P450 2B11 with that of P450 2B6 using a well-defined tumor cell population. It should be noted, however, that factors related to the efficiency of P450 gene delivery are likely to limit the extent of response that can be achieved *in vivo* using retroviral vectors, such as those employed in the present model studies. These limitations may, in part, be addressed by using replicating adenoviruses or other vectors for *in vivo* P450 2B11 delivery.

In conclusion, the present study shows the utility of the low K_m cyclophosphamide and ifosfamide 4-hydroxylase P450 2B11 for prodrug activation cancer gene therapy. The use of this enzyme in combination with P450R, coupled with a replication-conditional viral vector for gene delivery, may facilitate the development of more effective therapeutic approaches to cancer treatment.

[2] J. Ma and D.J. Waxman, unpublished experiments.

References

1. McKeown SR, Ward C, Robson T. Gene-directed enzyme prodrug therapy: a current assessment. Curr Opin Mol Ther 2004;6:421 – 35.
2. Shinohara ET, Lu B, Hallahan DE. The use of gene therapy in cancer research and treatment. Technol Cancer Res Treat 2004;3:479 – 90.
3. Dachs GU, Tupper J, Tozer GM. From bench to bedside for gene-directed enzyme prodrug therapy of cancer. Anticancer Drugs 2005;16:349 – 59.
4. Saukkonen K, Hemminki A. Tissue-specific promoters for cancer gene therapy. Expert Opin Biol Ther 2004;4:683 – 96.
5. McCormick F. Cancer-specific viruses and the development of ONYX-015. Cancer Biol Ther 2003;2:S157 – 60.
6. Brown JM, Wilson WR. Exploiting tumour hypoxia in cancer treatment. Nat Rev Cancer 2004;4:437 – 47.
7. Wei MX, Tamiya T, Chase M, et al. Experimental tumor therapy in mice using the cyclophosphamide-activating cytochrome P450 2B1 gene. Hum Gene Ther 1994;5:969 – 78.
8. Chen L, Waxman DJ. Intratumoral activation and enhanced chemotherapeutic effect of oxazaphosphorines following cytochrome P450 gene transfer: development of a combined chemotherapy/cancer gene therapy strategy. Cancer Res 1995;55:581 – 9.
9. Chen L, Waxman DJ. Cytochrome P450 gene-directed enzyme prodrug therapy (GDEPT) for cancer. Curr Pharm Des 2002;8:1405 – 16.
10. Rooney PH, Telfer C, McFadyen MC, Melvin WT, Murray GI. The role of cytochrome P450 in cytotoxic bioactivation: future therapeutic directions. Curr Cancer Drug Targets 2004;4:257 – 65.
11. Nakajima T, Wang RS, Nimura Y, et al. Expression of cytochrome P450s and glutathione *S*-transferases in human esophagus with squamous-cell carcinomas. Carcinogenesis 1996;17:1477 – 81.
12. Standop J, Schneider M, Ulrich A, Buchler MW, Pour PM. Differences in immunohistochemical expression of xenobiotic-metabolizing enzymes between normal pancreas, chronic pancreatitis and pancreatic cancer. Toxicol Pathol 2003;31:506 – 13.
13. Huang Z, Fasco MJ, Figge HL, Keyomarsi K, Kaminsky LS. Expression of cytochromes P450 in human breast tissue and tumors. Drug Metab Dispos 1996;24:899 – 905.
14. Murray GI, McFadyen MC, Mitchell RT, Cheung YL, Kerr AC, Melvin WT. Cytochrome P450 CYP3A in human renal cell cancer. Br J Cancer 1999;79:1836 – 42.
15. Jounaidi Y. Cytochrome P450-based gene therapy for cancer treatment: from concept to the clinic. Curr Drug Metab 2002;3:609 – 22.
16. Kan O, Kingsman S, Naylor S. Cytochrome P450-based cancer gene therapy: current status. Expert Opin Biol Ther 2002;2:857 – 68.
17. Hudis CA, Schmitz N. Dose-dense chemotherapy in breast cancer and lymphoma. Semin Oncol 2004;31:19 – 26.
18. Jounaidi Y, Hecht JED, Waxman DJ. Retroviral transfer of human cytochrome P450 genes for oxazaphosphorine-based cancer gene therapy. Cancer Res 1998;58:4391 – 401.
19. Chen L, Yu LJ, Waxman DJ. Potentiation of cytochrome P450/cyclophosphamide-based cancer gene therapy by coexpression of the P450 reductase gene. Cancer Res 1997;57:4830 – 7.
20. Jounaidi Y, Waxman DJ. Combination of the bioreductive drug tirapazamine with the chemotherapeutic prodrug cyclophosphamide for P450/P450-reductase-based cancer gene therapy. Cancer Res 2000;60:3761 – 9.
21. McErlane V, Yakkundi A, McCarthy HO, et al. A cytochrome P450 2B6 meditated gene therapy strategy to enhance the effects of radiation or cyclophosphamide when combined with the bioreductive drug AQ4N. J Gene Med 2005;7:851 – 9.
22. Jounaidi Y, Waxman DJ. Frequent, moderate-dose cyclophosphamide administration improves the efficacy of cytochrome *P*-450/cytochrome *P*-450 reductase-based cancer gene therapy. Cancer Res 2001;61:4437 – 44.
23. Browder T, Butterfield CE, Kraling BM, et al. Antiangiogenic scheduling of chemotherapy improves efficacy against experimental drug-resistant cancer. Cancer Res 2000;60:1878 – 86.
24. Ichikawa T, Petros WP, Ludeman SM, et al. Intraneoplastic polymer-based delivery of cyclophosphamide for intratumoral bioconversion by a replicating oncolytic viral vector. Cancer Res 2001;61:864 – 8.
25. Pawlik TM, Nakamura H, Mullen JT, et al. Prodrug bioactivation and oncolysis of diffuse liver metastases by a herpes simplex virus 1 mutant that expresses the CYP2B1 transgene. Cancer 2002;95:1171 – 81.
26. Jounaidi Y, Waxman DJ. Use of replication-conditional adenovirus as a helper system to enhance delivery of P450 prodrug-activation genes for cancer therapy. Cancer Res 2004;64:292 – 303.
27. Lohr M, Kroger J-C, Hoffmeyer A, et al. Safety, feasibility and clinical benefit of localized chemotherapy using microencapsulated cells for inoperable pancreatic carcinoma in a phase I/II trial. Cancer Ther 2003;1:121 – 31.
28. Salmons B, Lohr M, Gunzburg WH. Treatment of inoperable pancreatic carcinoma using a cell-based local chemotherapy: results of a phase I/II clinical trial. J Gastroenterol 2003;38 Suppl 15:78 – 84.
29. Braybrooke JP, Slade A, Deplanque G, et al. Phase I study of MetXia-P450 gene therapy and oral cyclophosphamide for patients with advanced breast cancer or melanoma. Clin Cancer Res 2005;11:1512 – 20.

30. Weber GF, Waxman DJ. Activation of the anti-cancer drug ifosphamide by rat liver microsomal P450 enzymes. Biochem Pharmacol 1993;45: 1685 – 94.

31. Huang Z, Roy P, Waxman DJ. Role of human liver microsomal CYP3A4 and CYP2B6 in catalyzing *N*-dechloroethylation of cyclophosphamide and ifosfamide. Biochem Pharmacol 2000;59:961 – 72.

32. Sladek NE. Metabolism and pharmacokinetic behavior of cyclophosphamide and related oxazaphosphorines. In: Powers G, editor. Anticancer drugs: reactive metabolism and interactions. United Kingdom: Pergamon Press; 1994. p. 79 – 156.

33. Furlanut M, Franceschi L. Pharmacology of ifosfamide. Oncology 2003;65:2 – 6.

34. Chen CS, Lin JT, Goss KA, He YA, Halpert JR, Waxman DJ. Activation of the anticancer prodrugs cyclophosphamide and ifosfamide: identification of cytochrome P450 2B enzymes and site-specific mutants with improved enzyme kinetics. Mol Pharmacol 2004;65:1278 – 85.

35. Monga M, Sausville EA. Developmental therapeutics program at the NCI: molecular target and drug discovery process. Leukemia 2002;16: 520 – 6.

36. Chen G, Waxman DJ. Identification of glutathione *S*-transferase as a determinant of 4-hydroperoxy-cyclophosphamide resistance in human breast cancer cells. Biochem Pharmacol 1995;49:1691 – 701.

37. Morgenstern JP, Land H. Advanced mammalian gene transfer: high titre retroviral vectors with multiple drug selection markers and a complementary helper-free packaging cell line. Nucleic Acids Res 1990;18: 3587 – 96.

38. Huang Z, Raychowdhury MK, Waxman DJ. Impact of liver P450 reductase suppression on cyclophosphamide activation, pharmacokinetics and antitumoral activity in a cytochrome P450-based cancer gene therapy model. Cancer Gene Ther 2000;7:1034 – 42.

39. Hasler JA, Harlow GR, Szklarz GD, et al. Site-directed mutagenesis of putative substrate recognition sites in cytochrome P450 2B11: importance of amino acid residues 114, 290, and 363 for substrate specificity. Mol Pharmacol 1994;46:338 – 45.

40. Pear WS, Nolan GP, Scott ML, Baltimore D. Production of high-titer helper-free retroviruses by transient transfection. Proc Natl Acad Sci U S A 1993;90:8392 – 6.

41. Hecht JED, Jounaidi Y, Waxman DJ. Construction of P450-expressing tumor cell lines using retroviruses. In: Walther W, Stein U, editors. Methods in Molecular Medicine series: gene therapy of cancer: methods and protocols. Totowa (NJ): Human Press, Inc.; 2000.

42. Finer MH, Dull TJ, Qin L, Farson D, Roberts MR. kat: a high-efficiency retroviral transduction system for primary human T lymphocytes. Blood 1994;83:43 – 50.

43. Huang Z, Waxman DJ. High-performance liquid chromatographic-fluorescent method to determine chloroacetaldehyde, a neurotoxic metabolite of the anticancer drug ifosfamide, in plasma and in liver microsomal incubations. Anal Biochem 1999;273:117 – 25.

44. Bohnenstengel F, Eichelbaum M, Golbs E, Kroemer HK. High-performance liquid chromatographic determination of acrolein as a marker for cyclophosphamide bioactivation in human liver microsomes. J Chromatogr B Biomed Sci Appl 1997;692:163 – 8.

45. Horwitz MS. Function of adenovirus E3 proteins and their interactions with immunoregulatory cell proteins. J Gene Med 2004;6 Suppl 1:S172 – 83.

46. O'Shea CC, Johnson L, Bagus B, et al. Late viral RNA export, rather than p53 inactivation, determines ONYX-015 tumor selectivity. Cancer Cell 2004;6:611 – 23.

47. Paine-Murrieta GD, Taylor CW, Curtis RA, et al. Human tumor models in the severe combined immune deficient (scid) mouse. Cancer Chemother Pharmacol 1997;40:209 – 14.

48. Kumar S, Chen CS, Waxman DJ, Halpert JR. Directed evolution of mammalian cytochrome P450 2B1: mutations outside of the active site enhance the metabolism of several substrates, including the anticancer prodrugs cyclophosphamide and ifosfamide. J Biol Chem 2005;280: 19569 – 75.

49. Yule SM, Price L, McMahon AD, Pearson AD, Boddy AV. Cyclophosphamide metabolism in children with non-Hodgkin's lymphoma. Clin Cancer Res 2004;10:455 – 60.

50. Busse D, Busch FW, Bohnenstengel F, et al. Dose escalation of cyclophosphamide in patients with breast cancer: consequences for pharmacokinetics and metabolism. J Clin Oncol 1997;15:1885 – 96.

51. Denny WA. Tumor-activated prodrugs—a new approach to cancer therapy. Cancer Invest 2004;22:604 – 19.

52. Waxman DJ, Schwartz PS. Harnessing apoptosis for improved anticancer gene therapy. Cancer Res 2003;63:8563 – 72.

53. Schwartz PS, Chen CS, Waxman DJ. Enhanced bystander cytotoxicity of P450 gene-directed enzyme prodrug therapy by expression of the antiapoptotic factor p35. Cancer Res 2002;62:6928 – 37.